American Journal of Electrical Power and Energy Systems
2023; 12(2): 32-39
http://www.sciencepublishinggroup.com/j/epes
doi: 10.11648/j.epes.20231202.12
ISSN: 2326-912X (Print); ISSN: 2326-9200 (Online)

Adaptive LMS MPPT Controller and Adaptive Inverter Control Law to Control the Solar Photovoltaic System

Nalini Karchi[1, *], Deepak Kulkarni[2]

[1]Department of Electrical and Electronics Engineering, KLE Dr. M. S. Sheshgiri College of Engineering & Technology, Belagavi, India
[2]Department of Electrical and Electronics Engineering, Gogte Institute of Technology, Belagavi, India

Email address:
nnnalini2000@rediff.com (Nalini Karchi), dbkulkarni@git.edu (Deepak Kulkarni)

[*]Corresponding author

To cite this article:
Nalini Karchi, Deepak Kulkarni. Adaptive LMS MPPT Controller and Adaptive Inverter Control Law to Control the Solar Photovoltaic System. *American Journal of Electrical Power and Energy Systems.* Vol. 12, No. 2, 2023, pp. 32-39. doi: 10.11648/j.epes.20231202.12

Received: August 17, 2022; **Accepted**: September 16, 2022; **Published**: June 5, 2023

Abstract: The objective of the proposed work is to develop the maximum power point tracking controller and inverter controller by applying the adaptive Least mean square algorithm to control the total harmonics distortion of a solar photovoltaic system. The advantage of the adaptive LMS algorithm is simple and required less computational time. The adaptive LMS algorithm is applied to modify the perturbation and observation, maximum power point tracking controller. In this controller, the adaptive LMS algorithm is used to predict solar photovoltaic power. The development of the inverter control law is done using the d-q frame theory. This helps to reduce the number of equations to build a control law. The load current, grid current and grid voltage are sensed and transformed into d and q components. This adaptive LMS control law is used to extract the reference grid currents and later compared them to the actual grid currents. The comparison result is used to generate the switching gate pulses for inverter switches. The proposed controllers are developed and implemented with a solar PV system in MATLAB Simulink. The total harmonics distortion in current and voltage is investigated under linear and non-linear load conditions with changes in solar irradiations. The analysis is done by selecting step incremental values and sampling time.

Keywords: Solar PV System, MPPT Controller, Inverter Controller, Adaptive Control Algorithm, Power Quality Issues

1. Introduction

The demand for electrical energy has increased due to industrial development and the modernization of society. The supply of additional electrical power to fulfill the requirements is mainly done by renewable energy-based distributed generation (DG) units. Among all, Solar energy-based generating units are popular due to the ample availability of sunlight. It is easy to convert solar energy into electrical energy by using a photovoltaic diode. The generated power by solar photovoltaic is dc power that needs to be converted into AC power as loads are AC loads. Many solar generating plants are interconnected to the grid to transmit the power as well as power factor improvement. The integration of the Solar photovoltaic system to the power grid causes power quality issues such as distortion in voltage and current waveforms, harmonics, voltage swag and swell, etc. Here power electronics play an important role in power conversion and transmission. The power converters are used to convert dc to ac power. Solar plants are interfaced with the grid through power electronics converters. The major advantage of power electronic devices is that it provides flexibility in control through the generation of switching pulses. Due to the involvement of power electronics devices, there are other power quality challenges in the connection of DG to the grid such as waveform distortion, harmonics, changes in impedance at the common coupling point [1, 2]. There are two main converters that are important in power conversion and transmission from the solar plant to the grid. These converters are DC-DC converter and DC-AC converter. The DC-DC converter is used at the output of a solar PV Panel to extract the maximum power by using the

Maximum Power Point controller. Several MPPT conventional controllers are available like perturbation and observation, incremental conductance, etc. The most widely used MPPT controller is P & O MPPT controller due to its simplicity and ease of implementation. Similarly, the DC-AC converter is located on the grid side. The input to this converter is from the dc-dc converter. The output of this converter is regulated by generating the proper sequence of gate pulses to the switches used in an inverter. The output of the converter is controlled by controlling the operation of the on and off state of the switches used in the converter. The most commonly Proportional Integral controller is used to control gate pulses to switches and the output of the DC-AC inverter. The parameters of the PI controller are fixed. The parameters don't adjust with the change in the load condition. The authors have explained the limitations of the PI controller to control the Solar PV system. Soft computing technologies such as particle swarm optimization, genetic algorithm, fuzzy logic, artificial neural network, grey wolf, fireflies, cuckoo search, etc. can be used for MPPT and inverter controllers. Still, it is hard to manage the computing time and complexity. Among MPPT controllers, the P & O controller is widely used because it is simple. But the output PV panel power fluctuates at the final operating point (maximum power point) [3].

In this paper, the MPPT and INVERTER controllers are developed using an Adaptive LMS algorithm. The P & O MPPT controller is modified using the LMS algorithm theory. The inverter control law is developed using the LMS algorithm as well as the d-q theory. The developed controllers are implemented to control the solar PV system. The total harmonic distortion is measured by the FFT tool in MATLAB under linear and non-linear load.

2. System Formation

The block of the system is shown in figure 1. The solar photovoltaic system is composed of a PV array panel, dc-dc boost converter, three-phase inverter, and L-filter [4].

2.1. Solar PV Panel

The basic electrical equivalent diagram is shown in figure 2. The PV panel is formed by the series and parallel connection of PV modules. For the case study, the power capacity of a Solar PV panel is 51kw with 406 V DC voltage. To obtain 51kW power from the panel, there are 17 parallel strings and 14 series modules per string in the PV array. The module configuration details are given in table 1. The selection of a number of series modules (Ns) is based on the voltage at the maximum power point, V_{mp} and output DC voltage, V_{dc}. The number of strings is determined by the current at the maximum power point, I_{mp} by (1), (2). P_{max} is the maximum power capacity to be maintained [4].

$$N_s = \frac{V_{dc}}{V_{mp}} \quad (1)$$

$$N_P = \frac{P_{max}/V_{dc}}{I_{mp}} \quad (2)$$

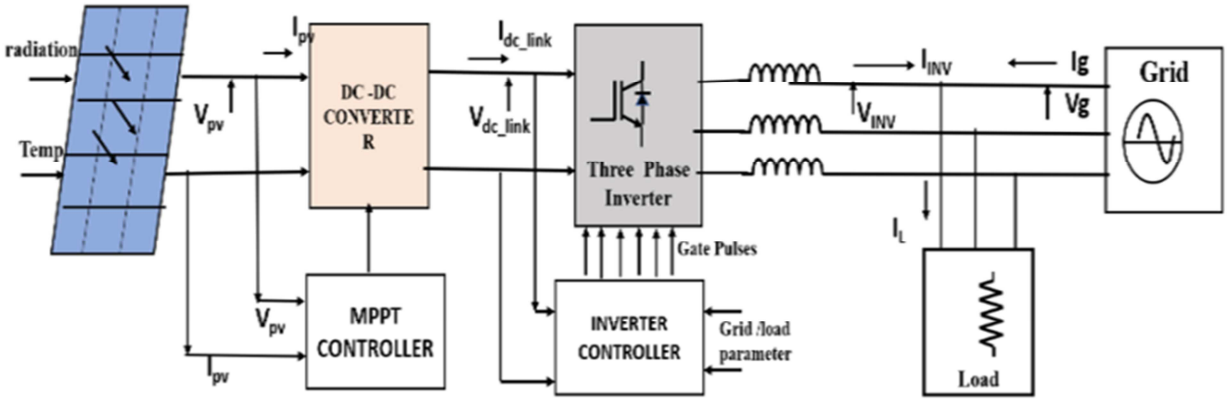

Figure 1. *Block diagram of Solar Photovoltaic System.*

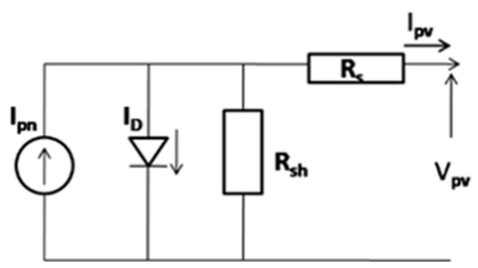

Figure 2. *The equivalent Electrical Circuit of PV Cell.*

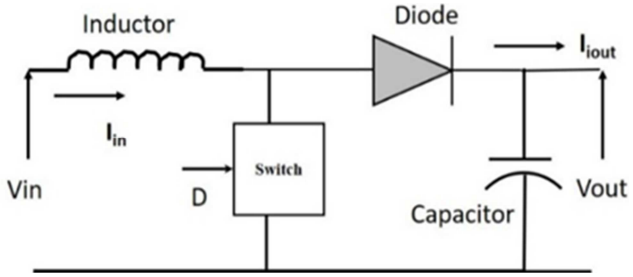

Figure 3. *The block diagram of the DC-DC boost converter.*

2.2. DC-DC Boost Converter

The basic functional block diagram is shown in figure 3. The output of the Solar PV Panel is given to the DC-DC converter. The function of this converter is to step up the input voltage to a higher level. The operation of the converter is based on the maximum power transfer theorem. It works on the impedance matching concept when the internal resistance of the PV panel and equivalent resistance of the DC-DC converter looking into the output terminals of the PV panel is matching to each other, the maximum power transfer can happen from the P V panel to the DC-DC converter. The working of the DC-DC converter is controlled by the duty cycle provided by the MPPT controller. The selection of DC-DC converter is obtained by (3), (4) and (5). D is known as the duty cycle. Vo is the output voltage of the boost converter, V_{in}, is the input voltage to the boost converter from the PV panel. ΔI is ripple factor in current and ΔV ripple factor in voltage. fsw, is the switching frequency of the converter switch [4].

$$D = 1 - \frac{v_{in}}{v_o} \tag{3}$$

$$L_{dclink} = \frac{V_{in}(V_o - V_{in})}{f_{sw}(\Delta I * V_o)} \tag{4}$$

$$C_{dclink} = \frac{I_{in}(V_o - V_{in})}{f_{sw}(\Delta V * V_o)} \tag{5}$$

2.3. Three-Phase Two-Level Inverter (DC-AC Converter)

In the following case study, the selected two-level three-phase inverter of 51kW power capacity is built by using six IGBT power electronics switches. The operation of IGBTs is controlled by the sinusoidal pulse width modulation (SPWM) technique. The AC output of the inverter is obtained by controlling the ON and OFF state of IGBT switches. This ON and OFF state of switches are managed by the proper generation of gate pulses of the switches through an inverter controller. The inverter AC output voltage is 380 V (line voltage).

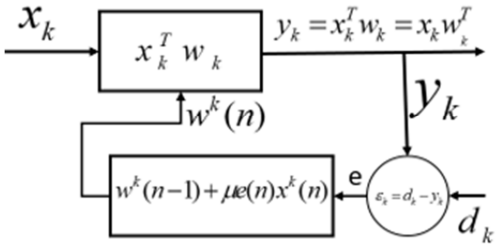

Figure 4. *Adaptive LMS FIR structure.*

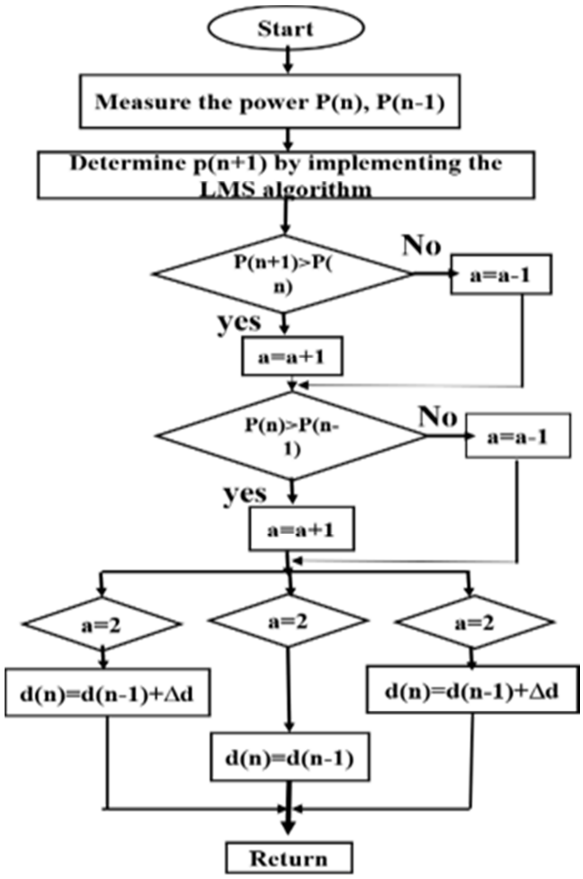

Figure 5. *Flow chart of adaptive LMS MPPT Controller.*

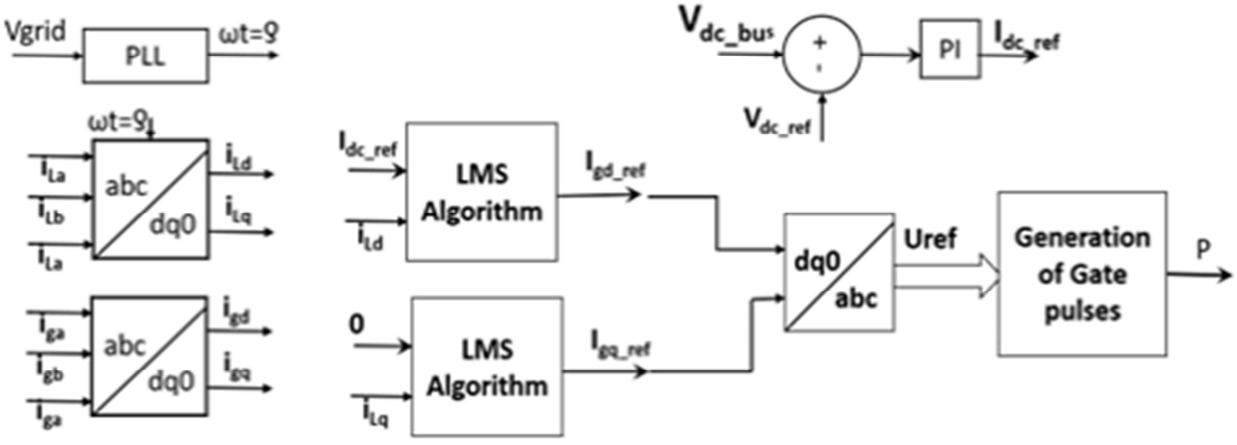

Figure 6. *Implementation of an Adaptive LMS Control law.*

3. Adaptive LMS Theory

The adaptive LMS implementation is shown in figure 4. The adaptive theory explains the updating of the weight values according to the changes in the system [6]. This weight updating depends on the error function. The weight values are changed to minimize the error function. The output function is managed by updating the weight function to minimize the error. The error is measured by comparing the actual output, y(n) and desired output, d(n). The optimized weight function, w(n) is found by finding the least mean square values of the error function, e(n). The adaptive LMS concept is explained in the equation (6), (7) and (8).

$$y(n) = w(n)^T x(n) \tag{6}$$

$$e(n) = d(n) - y(n) \tag{7}$$

$$w^k(n+1) = w^k(n) + \mu e(n) x^k(n) \tag{8}$$

$$|e(n)^2| = |(d(n) - y(n))|^2 \tag{9}$$

4. Control Scheme

The MPPT and Inverter controllers are two controllers which are important controllers to control the parameters on the solar PV panel and grid side respectively in the grid-connected solar PV system. The P&O MPPT controller is modified by applying the adaptive LMS algorithm as explained in section 3. The development of adaptive LMS MPPT is discussed in section 4.1 similarly, the adaptive LMS control law as an inverter controller in section 4.2.

4.1. Adaptive LMS MPPT Controller

P(n+1), the power is predicted by applying the adaptive LMS concept as explained in (11). The error is found by (10) and accordingly, the predicted power is determined by (11) to minimize the error [5]. The development of adaptive is shown in the flow chart, figure 5. The MPPT controller is used to obtain the duty cycle for reference voltage to extract the maximum power from the PV panel. μ is incremental step size in (11). Its value is between 0.1 to 0.2 [7-9].

$$e_p(n) = P(n) - P(n-1) \tag{10}$$

$$P(n+1) = P(n-1) + 2\,\mu\, e_p(n)\, P(n) \tag{11}$$

4.2. Adaptive LMS Control Law- An Inverter Controller

Instead of using the PI controller, the gate switching pulses are generated by using a control scheme based on an adaptive LMS algorithm so it is known as the adaptive LMS control law. the objective is to extract the fundamental component of the gate current and compare it to the actual grid current to reduce the harmonics in the grid current [11]. The development of control law is expressed in the figure 6. The grid voltage is sensed at the interconnection point of the grid, load and inverter. This voltage is converted into the α-β phase system. The phase angle ϱ is obtained by (12) and (13). V_α and V_β are alpha-beta components of grid voltage. The d-q components of load current and grid current with respect to phase angle ϱ are found by (14). The procedure is divided into four steps,

1) obtain the d-q component of grid voltage, grid current and load current,
2) determine the dc reference current from dc link voltages,
3) apply the adaptive LMS algorithm to extract the reference fundamental load current,
4) generating switching gate pulses by comparing steps 2 and 3.

$$\begin{bmatrix} V_\alpha \\ V_\beta \end{bmatrix} = \begin{bmatrix} V_a - \frac{V_b}{2} - \frac{V_c}{2} \\ \frac{\sqrt{3}V_b}{2} - \frac{\sqrt{3}V_c}{2} \end{bmatrix} \tag{12}$$

$$\rho = wt = cos^{-1}\left(\frac{V_a - \frac{V_b}{2} - \frac{V_c}{2}}{\frac{\sqrt{3}V_b}{2} - \frac{\sqrt{3}V_c}{2}}\right) \tag{13}$$

$$\begin{bmatrix} I_d \\ I_q \end{bmatrix} = \begin{bmatrix} cos\,\rho & sin\,\rho \\ -sin\,\rho & cos\,\rho \end{bmatrix} \begin{bmatrix} 1 & -1/2 & -1/2 \\ 0 & \frac{\sqrt{3}}{2} & \frac{-\sqrt{3}}{2} \end{bmatrix} \begin{bmatrix} I_a \\ I_b \\ I_c \end{bmatrix} \tag{14}$$

$$Id^* = V_{dce}.* K_p + K_I \int V_{dce} dt \tag{15}$$

$$V_{dce} = v_{dclink} - v_{dclink\,ref} \tag{16}$$

I_d is the DC reference current that is obtained from measured DC link voltage, $v_{dclink}$and the reference dc link voltage, $v_{dclink\,ref}$ [10]. The instantaneous error at kth instant is determined from sensed grid current and weighted current for the d-q component by applying the adaptive LMS algorithm concept in section 3. The weighted component of the load current has been evaluated (17), (18). W(n), weight function of load current. $e_i(n)$ is error between d- component of actual load current and d-component of reference current. β is step size in weight function. Similarly, q component of reference current is obtained by (20), (21) and (22). Iq is q-component of load current [12-16].

$$e_i(n) = I_d - w(n) I_{dc\_ref}(n) \tag{17}$$

$$w(n) = w(n-1) + \beta e_i(n) I_{dc\_ref}(n) \tag{18}$$

$$I_d(n) = w(n) I_d^*(n) \tag{19}$$

$$e_q(n) = I_q - w(n) I_q^*(n) \tag{20}$$

$$w(n) = w(n-1) + \eta e(n) I_q^*(n) \tag{21}$$

$$I_q(n) = w(n) I_q^*(n) \tag{22}$$

The generated reference components are transformed into a-b-c three-phase form. There are used to generate switching gate pulses for the multifunctional inverter [11, 15, 16].

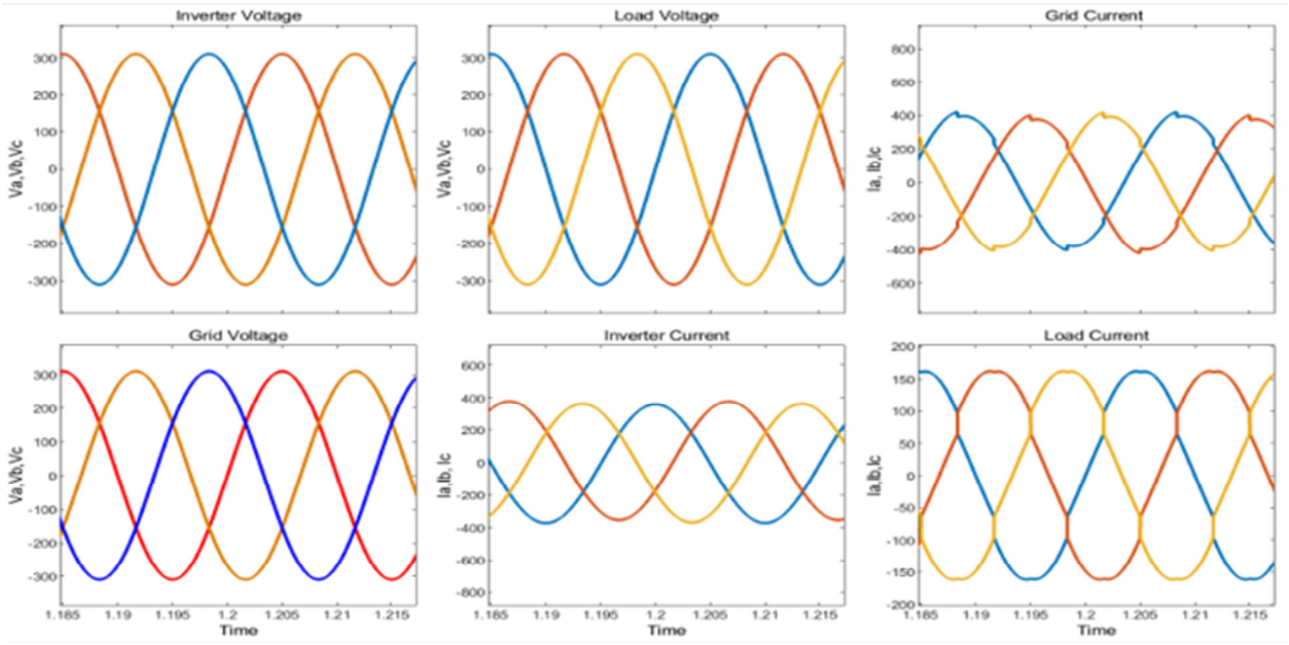

Figure 7. *Voltage and current performance of Solar PV system under nonlinear load (P=10kW and Q=200VAR) and variation solar radiation.*

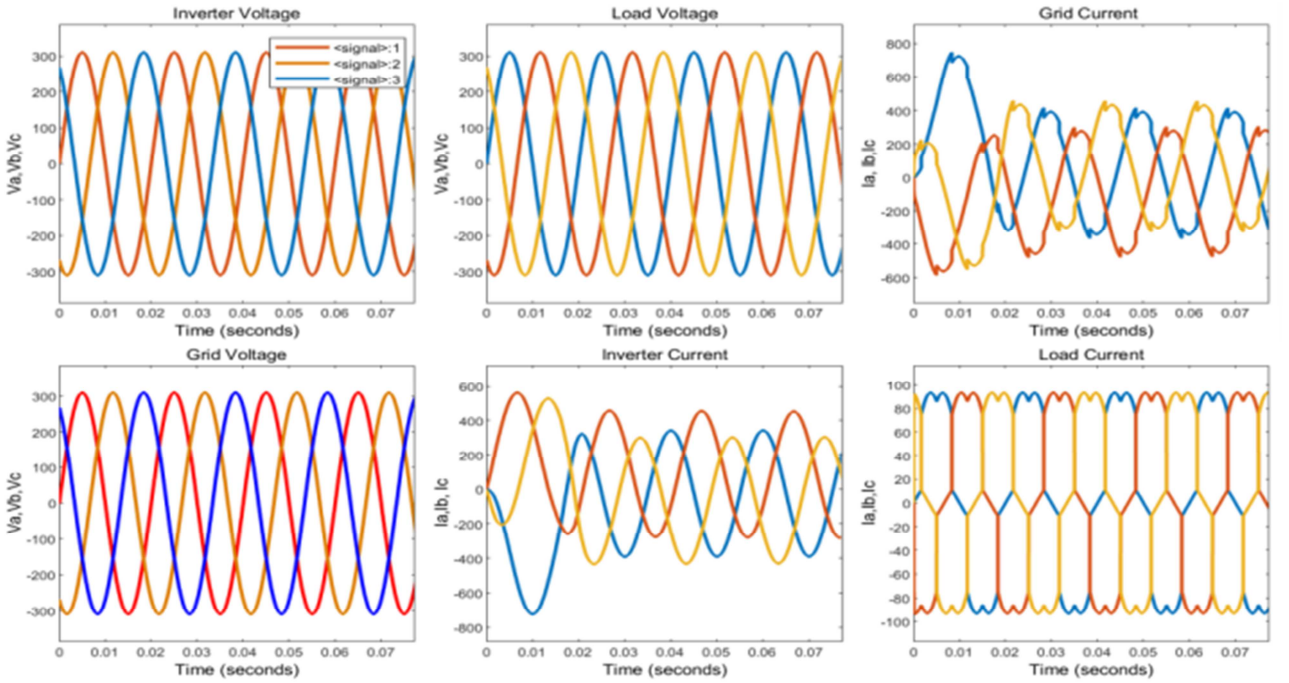

Figure 8. *Voltage and current performance of Solar PV system under nonlinear load and variation solar radiation under linear load =10kw, non- linear load (P=20kw and Q=100VAR) and variation solar radiation.*

Table 1. *Solar PV module Configuration.*

Module	Solon Solon Blue 220/01 215
Maximum power, (W)	214.97
Open circuit voltage, V_{oc}, (V)	36.18
Short circuit current, Isc, (A)	7.88
Voltage at maximim power point, V_{mp}, (V)	29.05
Current at maximum power point, I_{mp}, (A)	7.4
Internal series resistance, (ohms)	0.36428
Internal shunt resistance, (ohms)	407.0581

5. Result and Discussion

The adaptive LMS MPPT controller and adaptive control law are implemented for the control of the Solar PV System. The performance is observed for the condition given below:

1) Change in Non-linear load.
2) Input: variation in solar radiation.
3) Change in sampling time.
4) Change in step size.

Table 2. *Solar PhotoVoltaic System configurations.*

Parameters	Value
Sampling time, Tss, (sec)	50e-6 sec
Rated power, (W)	51e3
Grid voltage, (V)	380
Filter inductor. Lf, (H)	0.0027
Filter resistance, RLf, (ohm)	0.0676
DC boost converter input voltage, $V_{in,}$ (V)	406.2000
Voltage at maximum power point, Vmpp (V)	406.2000
DC votlage of DC boost converter, Vo, (V)	700
fsw_boost, (Hurtz)	5000
L_bound, (H)	1.3579e-04
L_boost, (H)	0.0014
C_boost, (Farad)	8.7369e-04

Table 3. *Total harmonic distortion in grid current with change in linear load, sampling time and step-size, solar radiation is varying from 0 to 1000 W/m^2.*

Non-linear Load	Step size	Sampling time (Sec)	Settling time (Sec)	Grid current. (THD in%)	Load current. (THD in%)
P=10kW and Q=200 VAR	0.0001	40µsec	---	6.30	23.85
P=10kW and Q=200VAr	0.001	40µsec	0.02	6.28	23.85
P=10kW and Q=200VAr	0.01	40µsec	0.0205	6.28	23.85
P=10kW and Q=100VAr	0.001	40µsec	0.525	3.22	19.88
P=10kW and Q=100VAr	0.001	50 µsec	0.8	2.95	7.14
P=10kW and Q=100VAr	0.01	50 µsec	0.9	2.95	7.14

Table 4. *Comparative Analysis for different load.*

Load	Grid Current harmonics (THD) in%	Load Current harmonics (THD) in%
Non-linear Load (10kW linear connected in parallel with Rectifier with R=10kW and Q=100VAR)	3.22	19.64
Non-linear Load (60kW linear connected in parallel with Rectifier with R=10kW and Q=100VAR)	2.95	7.11

Table 5. *Comparative Analysis for two different combinations of MPPT and Inverter controller non-linear Load (10kW linear connected in parallel with Rectifier with R=10kW and Q=100VAR) and Variation in solar radiation 0 to 1000W/m^2.*

Load	Grid Current harmonics (THD) in%	Load Current harmonics (THD) in%
Adaptive LMS Inverter control law and Perturb & Observe MPPT controller	4.75	19.89
Adaptive LMS Inverter control law and adaptive LMS MPPT controller	3.22	19.64

Table 6. *Comparison between d-q based LMS control algorithm and other adaptive control law with other author's results.*

Parameter / Adaptive technique Harmonics in %	i-PNLMS Based Control Algorithm	Novel power normalized kernel least mean fourth algorithm based neural network (NN) control (PNKLMF-NN) technique	Variable Step Size Least Mean Square Adaptive	variable parameter resized zero attracting least mean fourth (VP-RZA-LMF)	Wiener filtering based control algorithm	LMS, LMF and RLS to study the dynamic performance of PVDSTATCOM system	LMS adaptive control law
Grid Voltage	0.07	9.5	18.84	1.11	4.11	2.63	0%
Grid Current	4.9	2.4	4	3.1	4.61	3.63	3.22%
Load Current	27.14	36.8	29.39	24.53	23.89	NA	19.88%

The adaptive LMS MPPT controller and adaptive control law as inverter controller are implemented for the solar Photovoltaic system configured in table 2. The solar PV panel design details are given in table 1. The total harmonics distortion (THD in%) is investigated for different linear and nonlinear loads, sampling time and step size of weight updating. The controller performance is measured in terms of the settling time of the current response.

5.1. Variation in Input Solar Irradiation, Non-Linear, Sampling Time, Variation in Step-Size

The grid, load inverter current and voltage waveforms are sinusoidal in nature as shown in figures 7 and 8. The results are found better for step size 0.01 and 0.001 compared to 0.0001. The current response is stable for these two-step size values. It is also observed that the current response is stable when step size is between 0.01 to 0.9. The selected sampling time is 40µsec. For step size value less than 0.001 the current response is not settled at final value under nonlinear load (P=10 and Q=200 VAR) table 3. The THD of grid current and load current is measured as 6.28 and 23.85 respectively.

The sampling time is varied from 40µsec to 50µsec with constant step size of 0.001, the grid current THD is reduced from 3.22 to 2.5. similarly, the load current THD is reduced from 19.88 to 7.14%. Whereas the settling time is increased

from 0.525 sec to 0.8 sec with increased in sampling time. This is observed under the load condition (P=10kW and Q=100Var).

With change in step size from 0.001 to 0.01 and constant sampling time 50 μsec, the settling time is increased from 0.8 sec to 0.9 sec. There is no change in grid current and load current THD under load condition P=10kW and Q=100Var, table 3.

The selection of sampling time and step-size of the weight function is dependent on load condition. At the value of value μ=0.001 and sampling time 40 μsec, best tradeoff is observed in terms of reduction in total harmonics distortion in grid current and settling time of current response under (P=10 and Q=200 VAR). similarly, At the value of value μ=0.001 and sampling time 50 μsec, best tradeoff is observed in terms of reduction in total harmonics distortion in grid current and settling time of current response under (P=10 and Q=100 VAR).

5.2. Variation in Linear Load with Constant Solar Irradiation Input

With sampling time 40 μsec, input solar irradiation is constant 1000 W/m^2, step -size is 0.01, the grid current THD is reduced from 4.75 to 3.22% with increase in linear load as shown in Table 4. Similarly, there is more reduction in load current THD from 19.64 to 7.11%

5.3. Comparative Analysis for Two Different Combinations of MPPT and Inverter Controller

Comparative Analysis for two different combinations of MPPT and Inverter controller for non-linear Load (10kW linear connected in parallel with Rectifier with R=10kW and Q=100VAR) and Variation in solar radiation 0 to 1000W/m^2 is recorded in table 5. The adaptive LMS MPPT controller and inverter control law proves that there is reduction in grid and load current total harmonic distortion.

5.4. Comparative Analysis with Other Author Researcher Results

Comparative analysis results of proposed work and prior research work related adaptive LMS algorithm family's is shown in table 6.

6. Findings

The adaptive least mean square algorithm can be customized to develop the control law as well as MPPT controller. The adaptive LMS algorithm is simple and easy to implement for development of the controller. The adaptive control law has certain advantage over inverter PI controller. The effective results are dependent on selection of sampling time, step size of weight function, number of iterations in algorithm execution, switching frequency of dc-dc converter and inverter.

7. Conclusion

The adaptive LMS control law is developed using LMS algorithm. This algorithm uses the error function that determines the error between actual value and reference value. So, it saves burden of the random initialization of parameters. This algorithm is used in two ways in this proposed work firstly, to predict the PV power in adaptive LMS controller and extracting the reference grid current in adaptive control law. It is observed that voltage and current waveforms are sinusoidal in nature. The proper tradeoff between sampling time, step size of weight function, switching frequency need to be achieved to get effective results in reduction of total harmonic distortion of grid current and load current and reduce the settling time of response.

8. Future Scope

In proposed work the selected reference quadrature current is made equal to zero. This value can be found by using the actual grid voltage and reference grid voltage to achieve more precise result in reduction in total harmonic distortion in grid and load current. The LMS family algorithm can be applied to develop the controller.

References

[1] Iweh, C. D.; Gyamfi, S.; Tanyi, E.; Effah-Donyina, E. (2021). Distributed Generation and Renewable Energy Integration into the Grid: Prerequisites, Push Factors, Practical Options, Issues and Merits. Energies, 14, 5375. https://doi.org/10.3390/en141753

[2] Math H. J. Bollen, Fainan Hassan. (2018). Integration of Distributed Generation in the Power System. Wiley. reprint, ISBN: 978-81-265-7326-4.

[3] Harsh Patel, Rital Gajjar, Rajen Pandya, 'Artificial Intelligence Based MPPT techniques for Solar V System: A Review, Journal of Emerging Technologies and Innovative Research, 2019, ISSN-2349-5162.

[4] Pallavi Verma, Priya Mahajan et. al (2020). Smooth LMS-based adaptive control of SV system tied to the grid for enhanced power quality. *IET Power Electronics* September 2020.

[5] Obaidullah Lodin, Inderpreet Kaur, Harpreet Kaur. (2019) Predictive- P& O MPPT Algorithm for Fast and Reliable Tracking of Maximum Power Point in Solar Energy Systems. Journal of Recent Technology and Engineering (IJRTE), ISSN: 2277-3878, Volume-7, Issue-6S4, April 2019.

[6] Satish Choudhury and Byomakesh dash et al. (2020) Comparative Analysis of LMS Based Control Algorithms for Grid Integrated System Innovation. Electrical Power Engineering, Communication and Computing Technology Springer Nature, Singapore Pte Ltd. 2020, Lecture Notes in Electrical Engineering 630, doi.org/10.1007/978-981-15-2305-2_46.

[7] Sunaina Singh and Seema et al.. (2020). Adaptive based Leaky LMS Control Technique of Grid Connected SPV System. IEEE International Conference on Power Electronics, Drives and Energy Systems 978-1-7281-5672-9.

[8] Avdhesh Kumar and Rachana Garg et al. (2021). Control of Grid Integrated Photovoltaic System using new Variable Step size Least Mean Square adaptive filter. Springer Nature, March 2021.

[9] Manoj Badoni, Alka, Ankit Kumar Singh et al. (2020). Grid Tied Solar PV system with Power Quality Enhancement Using Adaptive Generalized Maximum Versoria Criterion. DOI: 10.17775/CSEEEJPES.2020.04820.

[10] Naki Guler and Erdal Irmak (2019). MPPT Based Model Predictive Control of Grid-Connected Inverter for PV Systems. International Conference Renewable Energy Research and Applications ICERER Brasov Romana 978-1-7281-3587-8/19.

[11] Eugene Walach and B. Widrow (1984). The least mean fourth LMF adaptive algorithm and its family. IEEE Transactions on Informative Theory.

[12] M Kalai Arasi and Dr. S Shivananaitha (2018). Harmonic Reduction by LMF Algorithm in Grid-Connected SPV System. 4th International Conference on Energy Efficient Technologies for Sustainability ICEETS18.

[13] Sachin Devassy and Bhim Singh. Design and Performance Analysis of Three-Phase Solar PV Integrated UPQC. 978-1-5090-0128-6/16-IEEE.

[14] Neha Beniwal and Ikhlaq et al. (2018). Implementation of DSTATCOM with i-PNLMS Based Control Algorithm under Abnormal Grid Conditions. IEEE Transactions on Industry Applications DOI: 10.1.1094/TIA.2018.

[15] Gunjan Varshney and Madhukar Dave et al. (2019). Unit Template-based Control of PV DSTATCOM. Recent Advances in Electrical and Electronics Engineering (Formerly Recent Patents on Electrical & Electronics Engineering) 12 1-7 DOI: 10.2174/2352096511665181081128 53.

[16] Rahul Kumar Agarwal and Ikhlaq Hussain et al. (2017) Application of LMS-Based NN Structure for Power Quality Enhancement in a Distribution Network Under Abnormal Conditions. IEEE Transactions on Neural Networks and Learning Systems DOI; 10.1109/TNNLS.2017.2677961.